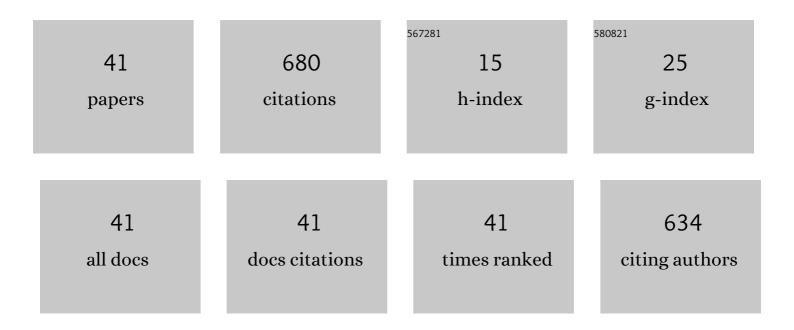
Atsushi Mahara

List of Publications by Year in descending order

Source: https://exaly.com/author-pdf/4347223/publications.pdf Version: 2024-02-01



#	Article	IF	CITATIONS
1	Tissue-engineered acellular small diameter long-bypass grafts withÂneointima-inducing activity. Biomaterials, 2015, 58, 54-62.	11.4	127
2	Continuous separation of cells of high osteoblastic differentiation potential from mesenchymal stem cells on an antibody-immobilized column. Biomaterials, 2010, 31, 4231-4237.	11.4	40
3	Tissue-engineered submillimeter-diameter vascular grafts for free flap survival in rat model. Biomaterials, 2018, 179, 156-163.	11.4	38
4	Complete Cell Killing by Applying High Hydrostatic Pressure for Acellular Vascular Graft Preparation. BioMed Research International, 2014, 2014, 1-7.	1.9	31
5	A surface graft polymerization process on chemically stable medical ePTFE for suppressing platelet adhesion and activation. Biomaterials Science, 2018, 6, 1908-1915.	5.4	29
6	<i>In vivo</i> guided vascular regeneration with a nonâ€porous elastinâ€like polypeptide hydrogel tubular scaffold. Journal of Biomedical Materials Research - Part A, 2017, 105, 1746-1755.	4.0	25
7	Design and characterization of a polymeric MRI contrast agent based on PVA for <i>in vivo</i> livingâ€cell tracking. Contrast Media and Molecular Imaging, 2010, 5, 309-317.	0.8	24
8	Anti-platelet adhesion and in situ capture of circulating endothelial progenitor cells on ePTFE surface modified with poly(2-methacryloyloxyethyl phosphorylcholine) (PMPC) and hemocompatible peptide 1 (HCP-1). Colloids and Surfaces B: Biointerfaces, 2020, 193, 111113.	5.0	24
9	The Rapid Inactivation of Porcine Skin by Applying High Hydrostatic Pressure without Damaging the Extracellular Matrix. BioMed Research International, 2015, 2015, 1-9.	1.9	22
10	Antibodyâ€immobilized column for quick cell separation based on cell rolling. Biotechnology Progress, 2010, 26, 441-447.	2.6	21
11	Preparation of Inactivated Human Skin Using High Hydrostatic Pressurization for Full-Thickness Skin Reconstruction. PLoS ONE, 2015, 10, e0133979.	2.5	21
12	Shortâ€ŧerm evaluation of thromboresistance of a poly(ether ether ketone) (PEEK) mechanical heart valve with poly(2â€methacryloyloxyethyl phosphorylcholine) (PMPC)â€grafted surface in a porcine aortic valve replacement model. Journal of Biomedical Materials Research - Part A, 2019, 107, 1052-1063.	4.0	21
13	Inactivation of Human Nevus Tissue Using High Hydrostatic Pressure for Autologous Skin Reconstruction: A Novel Treatment for Giant Congenital Melanocytic Nevi. Tissue Engineering - Part C: Methods, 2015, 21, 1178-1187.	2.1	18
14	Label-Free Separation of Induced Pluripotent Stem Cells with Anti-SSEA-1 Antibody Immobilized Microfluidic Channel. Langmuir, 2017, 33, 1576-1582.	3.5	18
15	Direct surface modification of metallic biomaterials via tyrosine oxidation aiming to accelerate the reâ€endothelialization of vascular stents. Journal of Biomedical Materials Research - Part A, 2018, 106, 491-499.	4.0	18
16	Accelerated endothelialization and suppressed thrombus formation of acellular vascular grafts by modifying with neointima-inducing peptide: A time-dependent analysis of graft patency in rat-abdominal transplantation model. Colloids and Surfaces B: Biointerfaces, 2019, 181, 806-813.	5.0	18
17	Design of in situ porcine closed-circuit system for assessing blood-contacting biomaterials. Journal of Artificial Organs, 2018, 21, 317-324.	0.9	15
18	Endothelial cell adhesion and blood response to hemocompatible peptide 1 (HCP-1), REDV, and RGD peptide sequences with free N-terminal amino groups immobilized on a biomedical expanded polytetrafluorethylene surface. Biomaterials Science, 2021, 9, 1034-1043.	5.4	14

Atsushi Mahara

#	Article	IF	CITATIONS
19	Verification of the Inactivation of Melanocytic Nevus in vitro Using a Newly Developed Portable High Hydrostatic Pressure Device. Cells Tissues Organs, 2016, 201, 170-179.	2.3	13
20	Arg-Glu-Asp-Val Peptide Immobilized on an Acellular Graft Surface Inhibits Platelet Adhesion and Fibrin Clot Deposition in a Peptide Density-Dependent Manner. ACS Biomaterials Science and Engineering, 2020, 6, 2050-2061.	5.2	13
21	Phospholipid polymer-based antibody immobilization for cell rolling surfaces in stem cell purification system. Journal of Biomaterials Science, Polymer Edition, 2014, 25, 1590-1601.	3.5	12
22	The superiority of the autografts inactivated by high hydrostatic pressure to decellularized allografts in a porcine model. Journal of Biomedical Materials Research - Part B Applied Biomaterials, 2017, 105, 2653-2661.	3.4	12
23	The Alteration of the Epidermal Basement Membrane Complex of Human Nevus Tissue and Keratinocyte Attachment after High Hydrostatic Pressurization. BioMed Research International, 2016, 2016, 1-9.	1.9	11
24	Modification of decellularized vascular xenografts with 8â€arm polyethylene glycol suppresses macrophage infiltration but maintains graft degradability. Journal of Biomedical Materials Research - Part A, 2020, 108, 2005-2014.	4.0	11
25	Small-Diameter Synthetic Vascular Graft Immobilized with the REDV Peptide Reduces Early-Stage Fibrin Clot Deposition and Results in Graft Patency in Rats. Biomacromolecules, 2020, 21, 3092-3101.	5.4	10
26	Impact of REDV peptide density and its linker structure on the capture, movement, and adhesion of flowing endothelial progenitor cells in microfluidic devices. Materials Science and Engineering C, 2021, 129, 112381.	7.3	10
27	Melanin pigments in the melanocytic nevus regress spontaneously after inactivation by high hydrostatic pressure. PLoS ONE, 2017, 12, e0186958.	2.5	10
28	An evaluation of the engraftment and the blood flow of porcine skin autografts inactivated by high hydrostatic pressure. , 2017, 105, 1091-1101.		8
29	Exploration of the Pressurization Condition for Killing Human Skin Cells and Skin Tumor Cells by High Hydrostatic Pressure. BioMed Research International, 2020, 2020, 1-17.	1.9	7
30	Cellular attachment behavior on biodegradable polymer surface immobilizing endothelial cell-specific peptide. Journal of Biomaterials Science, Polymer Edition, 2020, 31, 1475-1488.	3.5	6
31	Identification of circulating cells interacted with integrin α4β1 ligand peptides REDV or HGGVRLY. Peptides, 2021, 136, 170470.	2.4	5
32	<scp>REDV</scp> â€modified decellularized microvascular grafts for arterial and venous reconstruction. Journal of Biomedical Materials Research - Part A, 2022, 110, 547-558.	4.0	5
33	Superfine Magnetic Resonance Imaging of the Cerebrovasculature Using Selfâ€Assembled Branched Polyethylene Glycol–Gd Contrast Agent. Macromolecular Bioscience, 2018, 18, e1700391.	4.1	4
34	Adhesion of Flk1-expressing cells under shear flow in phospholipid polymer-coated immunoaffinity channels. Journal of Micromechanics and Microengineering, 2021, 31, 045012.	2.6	4
35	Accelerated tissue regeneration in decellularized vascular grafts with a patterned pore structure. Journal of Materials Chemistry B, 2022, 10, 2544-2550.	5.8	4
36	Visualising brain capillaries in magnetic resonance images <i>via</i> supramolecular self-assembly. Chemical Communications, 2020, 56, 11807-11810.	4.1	3

Atsushi Mahara

#	Article	IF	CITATIONS
37	High Hydrostatic Pressure Therapy Annihilates Squamous Cell Carcinoma in a Murine Model. BioMed Research International, 2020, 2020, 1-9.	1.9	3
38	A Novel Treatment for Giant Congenital Melanocytic Nevi Combining Inactivated Autologous Nevus Tissue by High Hydrostatic Pressure and a Cultured Epidermal Autograft: First-in-Human, Open, Prospective Clinical Trial. Plastic and Reconstructive Surgery, 2021, 148, 71e-76e.	1.4	3
39	Influence of Molecular Mobility on Contrast Efficiency of Branched Polyethylene Glycol Contrast Agent. Contrast Media and Molecular Imaging, 2018, 2018, 1-8.	0.8	1
40	Simple and efficient method for consecutive inactivation–cryopreservation of porcine skin grafts. Journal of Artificial Organs, 2020, 23, 147-155.	0.9	1
41	8. Polymeric MR Contrast Agents for Microvascular Imaging. Japanese Journal of Radiological Technology, 2022, 78, 520-525.	0.1	0